Nanoscale

View Online
Dynamic Article Links

Cite this: *Nanoscale*, 2011, **3**, 1383

www.rsc.org/nanoscale

FEATURE ARTICLE

Surfactant-assisted, shape-controlled synthesis of gold nanocrystals

Junyan Xiao and Limin Qi*

Received 30th October 2010, Accepted 20th December 2010
DOI: 10.1039/c0nr00814a

The shape control of gold nanocrystals has attracted extensive research interest because of their unique shape-dependent properties and widespread applications. Surfactants have been frequently used in the shape-controlled synthesis of gold nanocrystals in solution. In this feature article, we summarize some of the emerging colloidal approaches towards shape-tailored gold nanocrystals with the assistance of surfactants, focusing on the roles played by surfactants in shape control. We start with a discussion on the general strategies in shape control of gold nanocrystals, which include adsorbate-directed synthesis, seed-mediated synthesis, template-assisted synthesis, and the control of growth kinetics. Then, we highlight some recent progress in the gold nanocrystal synthesis assisted by single surfactants, mixed surfactants, supramolecular surfactants, as well as metal–surfactant complex templates, which is followed by a brief description of the potential applications of shaped gold nanocrystals in catalysis and molecular sensing.

1. Introduction

There has been a widespread and rapidly increasing interest in gold nanocrystals owing to their unique physical, chemical, and biocompatible properties, as well as promising applications in catalysis, sensing, bioimaging, photothermal therapy, drug delivery, nanoelectronics, and in the fabrication of photonic and plasmonic devices.[1–12] Gold nanocrystals have shown great potential in nanocatalysis where the catalytic efficiencies are size- and shape-dependent.[13] More interestingly, as typical plasmonic nanocrystals, gold nanocrystals exhibit unique optical properties. They can strongly absorb and scatter light through the collective oscillation of conduction band electrons confined within the nanocrystals, which is widely known as localized surface plasmon resonance (LSPR). Due to the plasmonic confinement, the optical properties of gold nanocrystals are highly dependent on their size, shape, structure, surroundings, and assembly pattern.[14] Furthermore, the cellular uptake of gold nanocrystals, which is essential in biological and biomedical applications, largely depends on their size and shape.[14] Therefore, there has been tremendous progress over the past decade in the shape-controlled synthesis of gold nanocrystals, and the investigation on their shape-dependent properties.[15–18]

Beijing National Laboratory for Molecular Sciences (BNLMS), State Key Laboratory for Structural Chemistry of Unstable and Stable Species, College of Chemistry, Peking University, Beijing, 100871, P. R. China. E-mail: liminqi@pku.edu.cn

Junyan Xiao

Junyan Xiao is currently a PhD student in Prof. Limin Qi's group at the College of Chemistry and Molecular Engineering, Peking University. She received her BS degree from the Department of Chemistry and Chemical Engineering, Huazhong University of Science and Technology (Hubei, China) in 2009. Her current research interests include controllable synthesis of novel metal nanostructures and their controllable assembly into advanced structures.

Limin Qi

Limin Qi received his PhD degree in Physical Chemistry from Peking University in 1998. He then went to the Max Planck Institute of Colloids and Interfaces to work as a postdoctoral fellow. In 2000, he joined the College of Chemistry at Peking University, where he has been a full professor since 2004. His current research focuses on the controlled synthesis and hierarchical assembly of functional micro- and nanostructures by colloidal chemical methods as well as bio-inspired approaches.

While a great deal of effort has been devoted to the size-controlled synthesis of spherical and pseudospherical gold nanocrystals through traditional colloidal routes, remarkable success has been achieved recently in the wet chemical synthesis of nonspherical gold nanocrystals with various sizes and shapes. In particular, a variety of colloidal chemical methods have been developed to fabricate gold nanocrystals with specific shapes, including rods,[19,20] wires,[21,22] belts,[23,24] combs,[24] plates and prisms,[25,26] polyhedra,[27–31] cages and frames,[32] caps,[33] stars and flowers,[13,34–37] as well as dendrites.[38–42] However, it remains a great challenge to fully elucidate the synthesis mechanisms and to realize the systematic, high-yield fabrication of these structures in a rational way. Among various anisotropic gold nanostructures, gold nanorods[43,44] and triangular nanoprisms[45] have received significant attention, and reliable methods have been established to make them in high yield with excellent control over structural parameters, which have been summarized in several recent reviews. Meanwhile, gold nanocrystals adopting the morphology of platonic polyhedra, which include tetrahedrons, octahedrons, cubes, icosahedrons, and dodecahedrons, have also attracted considerable attention.[27–30] Recently, polyhedral gold nanocrystals exhibiting high-index facets[46–51] and branched gold nanocrystals with tips (*e.g.* stars, flowers, and dendrites)[34–42,52] have been attracting increasing interest because of their promising applications in catalysis, plasmonics, and surface-enhanced Raman scattering (SERS).

In the shape-controlled synthesis of gold nanocrystals, various surfactants, which are amphiphilic molecules generally consisting of at least one hydrophilic head group and one hydrophobic chain, have been widely employed as capping agents to exert exquisite control over the nucleation and growth of gold nanocrystals. Particularly, cetyltrimethylammonium bromide (CTAB) is the most frequently used surfactant for the synthesis of gold nanorods in aqueous solution. In addition to the role of capping agents, surfactants which undergo strong interactions with gold can also significantly influence the growth kinetics of gold nanocrystals, which considerably influences the morphology of the final products, and can even form coordination complexes with gold that act as templates to direct the growth of shaped gold nanocrystals. Until now, a variety of surfactants with different headgroups, hydrophobic chains, counterions, and molecular architectures, have been used for the shape-controlled synthesis of gold nanocrystals. In this feature article, we summarize some of the emerging colloidal approaches towards shape-tailored gold nanocrystals with the assistance of surfactants, focusing on the roles played by surfactants in shape control. After a discussion of the general strategies in shape control of gold nanocrystals, we highlight some recent progress in gold nanocrystal synthesis assisted by single surfactants, mixed surfactants and supramolecular surfactants, as well as metal–surfactant complex templates, which is followed by a brief description of the potential applications of shaped gold nanocrystals.

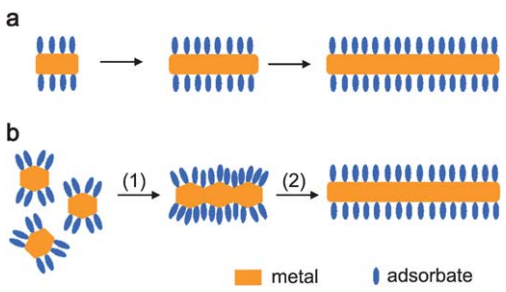

Fig. 1 Schematic illustration of the adsorbate-directed formation of metal nanorods through (a) directed growth and (b) oriented attachment.

2. General strategies in shape control of gold nanocrystals

Before the discussion of the surfactant-assisted synthesis of gold nanocrystals with tailored morphologies, we introduce some general strategies for controlling the shape of gold nanocrystals in colloidal synthesis. Surfactants may not be involved in all of these strategies, but surfactants usually affect the nanocrystal synthesis through one or several of them in the surfactant-assisted approaches.

2.1 Adsorbate-directed synthesis

In the colloidal synthesis of gold nanocrystals, shape control is achieved by accurately tuning the nucleation and growth processes, which may be under either thermodynamic or kinetic control. When crystal growth is under thermodynamic control, surface energy plays a crucial role in determining the morphology of gold nanocrystals since the surface-area-to-volume ratio is high for nanoparticles, and a crystal in equilibrium tends to have the lowest surface energy for a given volume of material. For colloidal synthesis, shape control at the crystallographic level can be achieved by employing molecular adsorbates that selectively adsorb to specific crystal planes, lowering the surface energy of these planes and thus stabilizing these facets.[16] A wide variety of molecules including surfactants, polymers, biomolecules, small organic molecules, and metal ions or atoms can act as crystallographically selective adsorbates to direct shape control of gold nanocrystals.

Basically, there are two different mechanisms for the adsorbate-directed synthesis of metal nanocrystals, namely directed growth and oriented aggregation. In the directed growth mechanism, the crystal growth through continuous addition of metal atoms is blocked on the crystal planes strongly bound by adsorbate molecules, and promoted on the crystal planes where there is no or weak binding. On the other hand, metal nanocrystals can be shaped through an oriented attachment mechanism where the preformed seeds selectively bound by adsorbate molecules undergo oriented attachment along the crystal planes where there is no or weak binding. Fig. 1 schematically illustrates the adsorbate-directed formation of metal nanorods through these two mechanisms. As shown in Fig. 1a, continuous addition of metal atoms to the exposed facets at two opposite ends leads to the formation of one-dimensional (1D) metal nanorods. As a typical example, Murphy and co-workers proposed that penta-twinned, [110]-oriented gold nanorods can be produced in a CTAB solution through selective adsorption of CTAB on the lateral {100} planes that are parallel to the [110] direction.[53] Alternatively, Liu and Guyot-Sionnest proposed that single-crystalline [100]-oriented gold nanorods can be obtained in CTAB solution through selective underpotential deposition

(UPD) of Ag adatoms on the gold {110} planes in the presence of Ag^+ ions.[54]

On the other hand, oriented attachment of preformed seeds along exposed facets at two opposite ends (step 1) and the subsequent sintering (step 2) lead to the formation of metal nanowires with smooth sides (Fig. 1b). In an original work, Halder and Ravishankar reported the seed-mediated synthesis of ultrathin Au nanowires in toluene in the presence of oleylamine and oleic acid.[55] They found that the oleylamine-capped Au seeds underwent oriented attachment along the oleylamine-free {111} facets, leading to branched gold structures; then, a room temperature sintering process of the attached Au nanocrystals occurred, resulting in the formation of the final [111]-oriented gold nanowires with smooth sides. While the oriented attachment-based synthesis sounds attractive for growing metal nanowires, the directed growth-based synthesis has been much more widely used and it can be readily extended to the synthesis of various metal nanostructures other than 1D structures.

2.2 Seed-mediated synthesis

In a typical synthesis of metal nanocrystals, the formation process of the final nanocrystals can be roughly divided into three distinct stages: 1) nucleation, 2) evolution of nuclei into seeds, and 3) growth of seeds into nanocrystals.[17] Here seeds can be viewed as nascent, faceted nanocrystals somewhat larger than nuclei, which keep a relatively stable structure during subsequent crystal growth. In a one-pot synthesis, the crystal seeds are formed *in situ* in the reaction mixture; alternatively, in a two-step synthesis, crystal seeds are prepared first and then the preformed seeds are added into the growth solution, which is called seed-mediated synthesis. While the one-pot synthesis is more convenient, the seed-mediated synthesis effectively isolates seed formation and growth as separate synthetic steps, which is particularly advantageous as it allows rational design of nanocrystal shape through the choice of seed structure and growth conditions.

Once a seed is formed, it can grow in size through the addition of metal atoms and thus the shape of the final nanocrystal is largely determined by the structure of the seed. A one-to-one correlation between the initial seeds and final nanocrystals has been established for a number of noble metals with the fcc structure, which is summarized in Fig. 2.[17,56] Generally, from single-crystal seeds, octahedrons, cuboctahedrons, or cubes will be produced, depending on the relative growth rates along the <111> and <100> directions. If uniaxial growth is somehow induced (for example, by selective adsorption of surfactants), the cuboctahedral and cubic seeds will grow into octagonal rods and rectangular bars, respectively. From singly twinned seeds, right bipyramids enclosed by {100} facets will be produced, which can also evolve into nanobeams. From multiply twinned seeds, icosahedrons, decahedrons, and pentagonal nanorods can be produced. Finally, when the seeds contain stacking faults, they will grow into thin plates, with the top and bottom faces being {111} facets.

If the seed structure and the growth condition are thoughtfully adjusted, the shape of the obtained nanocrystals can be readily adjusted. For example, two kinds of gold crystal seeds are widely

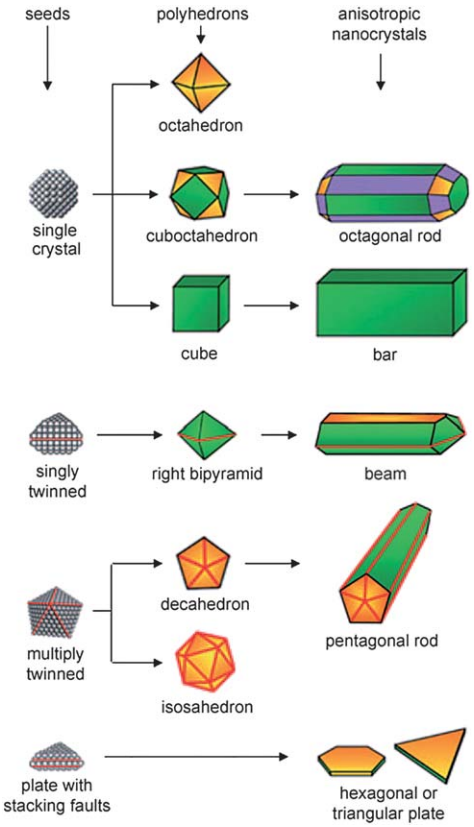

Fig. 2 Schematic illustration of the evolution pathways from fcc metal seeds with different structures to shaped nanocrystals. The green, orange, and purple colors represent the {100}, {111}, and {110} facets, respectively. Twin planes are delineated in the drawing with red lines. Reprinted with permission from ref. 56, copyright 2007 Wiley-VCH Verlag GmbH & Co.

used in gold nanocrystal synthesis. One is citrate-capped, penta-twinned particles bound by {111} facets, and the other is CTAB-capped single-crystal particles with a pseudospherical shape. If the single-crystal particles were adopted as seeds, single-crystalline [100]-oriented gold nanorods were obtained in CTAB solution in the presence of Ag^+ ions.[54] If the penta-twinned particles were used as seeds, penta-twinned, [110]-oriented gold nanorods were produced in CTAB solution without Ag^+ ions,[53] whereas bipyramidal gold nanocrystals were obtained in CTAB solution in the presence of Ag^+ ions.[54]

2.3 Template-assisted synthesis

The use of spatially and dimensionally constrained structures as templates is an effective method to prepare metal nanocrystals with a morphology similar or complementary to that of the template. Both hard and soft templates can be employed for the shape-controlled synthesis of gold nanocrystals. For example, porous aluminium oxide membranes containing uniform cylindrical pores can be used as hard templates for the electrochemical preparation of gold nanorods, which may represent one of the first major developments in high-yield, solution-phase synthesis of anisotropic metallic nanostructures.[57] This membrane-based approach is very useful for synthesizing metal nanorods with

control over both diameter and length. Recently, novel plasmonic nanorod metamaterials for biosensing were prepared by electrochemical growth of gold nanorod arrays using a substrate-supported, thin-film porous aluminium oxide template.[58] In addition to the synthesis of 1D gold nanostructures, gold nanocrystals with complex morphologies, such as branched[59] and cap-like[33] particles, can be produced by employing suitable hard templates. On the other hand, some flexible structures assembled by surfactants can be utilized as soft templates for synthesizing gold nanowires. As a representative example, single-crystal gold nanowires with a diameter of 1.6 nm were synthesized by ageing the oleylamine solution of $HAuCl_4$ at room temperature, where the mesostructures formed by cooperative assembly between the Au^+ ions and oleylamine were believed to serve as growth templates and govern anisotropic growth in the nanoscale.[60]

In addition to the traditional templates acting as spatially confined reaction media, certain reactive solids with a specific shape can be used as sacrificial templates for the production of metal nanocrystals, which adopt the underlying shape of the template. In particular, Ag nanocubes can be used as sacrificial templates for the fabrication of novel Au nanocages and nanoframes through a galvanic displacement reaction (Fig. 3).[32] With the addition of $HAuCl_4$ solution into a boiling suspension of Ag nanocubes, a pinhole is formed on one of the six faces, and gold is deposited epitaxially on the surface of the Ag cube. As the Au layer forms, the initial pinhole serves as the site for Ag dissolution, facilitating the conversion of the nanocube into a Au/Ag alloyed nanobox. With the addition of more $HAuCl_4$ solution, dealloying occurs, resulting in the formation of a porous gold nanocage with an underlying cubic form. By using the wet etchant $Fe(NO_3)_3$ to selectively dissolve Ag from the Au/Ag alloyed nanobox, a unique gold nanoframe is obtained.

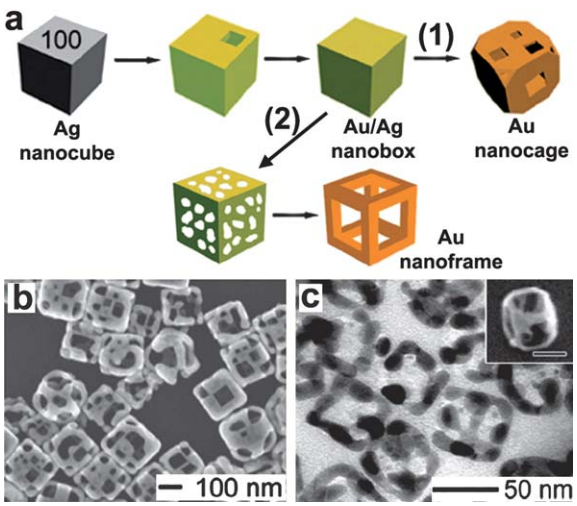

Fig. 3 (a) Schematic illustration of the formation of Au nanocages and nanoframes from an Ag nanocube that serves as a template. Coloration indicates the conversion of an Ag nanocube into an Au/Ag nanocage *via* galvanic replacement, and then into Au nanocages *via* continued galvanic replacement (1) or an Au nanoframe *via* selective etching with a wet etchant (2). SEM and TEM images of Au nanocages (b) and nanoframes (c). Reprinted with permission from ref. 32, copyright 2008 American Chemical Society.

Representative scanning electron microscopy (SEM) and transmission electron microscopy (TEM) images of the obtained Au nanocages and nanoframes are shown in Fig. 3.

2.4 Control of growth kinetics

The final shape of metal nanocrystals can be significantly influenced by the growth kinetics of the crystal nuclei. In general, isotropic growth of nanocrystals into the thermodynamically favored equilibrium morphologies is preferred under a thermodynamically controlled regime, whereas anisotropic growth of nanocrystals into a shape which deviates from the equilibrium morphology is facilitated under a kinetically controlled regime.[61] The main criterion proposed to achieve kinetic control is that the reaction should proceed considerably slower than under normal conditions. In practice, kinetically controlled synthesis can be achieved by substantially slowing down the precursor decomposition or reduction.[17] Kinetic control refers to the formation of crystals under conditions away from thermodynamic equilibrium, *i.e.* when a finite driving force exists for the formation of the crystal. The kinetic control regimes can be further divided based on the thermodynamic driving force available for the crystal growth. For the kinetically controlled synthesis of gold nanocrystals, two-dimensional (2D) plate-like nanostructures are obtained at a low driving force, while star-shaped or dendritic nanostructures are produced at a high driving force, *i.e.* far away from equilibrium.[61] It is worth noting that for reactions occurring far from equilibrium, a small change in reaction condition amplifies the differences in surface energies and hence the growth rates of individual facets, and the differences can be further amplified by exploiting the selective adsorption of capping agents on different facets.

Fig. 4 summarizes the possible evolution from fcc metal seeds to stars and dendrites under a kinetically controlled synthesis. From triangular plate seeds, planar tripods with each arm extending along either the <211> or <110> direction can be formed.[62,63] Under suitable conditions, planar dendrites, with the <111>-oriented trunk and branches, can be formed.[39] From penta-twinned decahedron seeds, planar pentapods, with each arm extending along either the [211] or [110] direction, can be formed.[13] From cubic seeds, fast growth along the <111> direction results in tetrapods with each arm extending along the <111> direction, which may further evolve into three-fold symmetric dendrites with <111>-oriented trunk and branches.[38] Similarly, from octahedron seeds, fast growth along the <100> direction may result in hexapods with each arm extending along the <100> direction, which could further evolve into four-fold symmetric dendrites with a <100>-oriented trunk and branches. Finally, from polycrystalline or multiply twined particles with surface asperities, irregular stars are formed.[35]

Recently, we have successfully synthesized hierarchical, three-fold symmetric, single-crystalline gold dendrites by a reaction between zinc plate and a solution of $HAuCl_4$ in the ionic liquid 1-butyl-3-methylimidazolium hexafluorophosphate ([BMIM][PF_6]). As shown in Fig. 5, these unique dendritic gold nanostructures exhibit a three-order hierarchy, *i.e.* a threefold symmetric <111>-oriented trunk, three groups of trident-like <111>-oriented branches grown on the trunk, and many <111>-oriented nanorod leaves grown on the branches symmetrically, indicating an

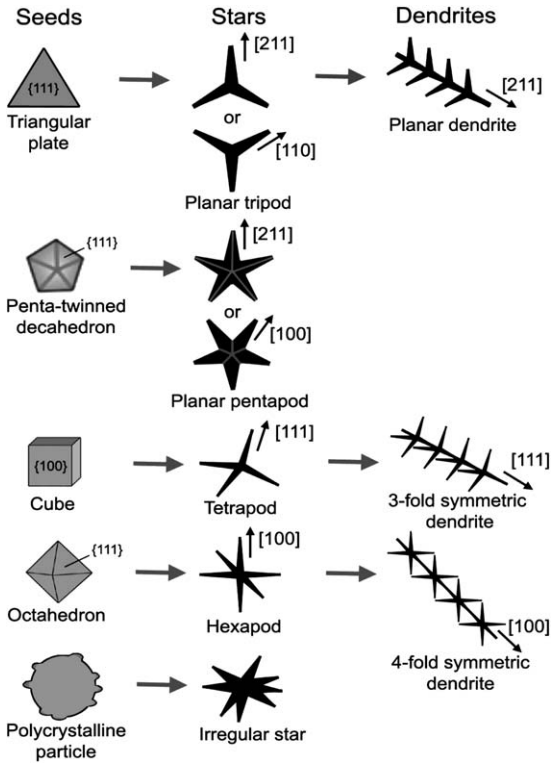

Fig. 4 Schematic illustration of the possible evolution from fcc metal seeds to stars and dendrites under kinetically controlled synthesis.

interesting fractal growth. It was proposed that the significantly lowered ion diffusivity and reaction rate in the ionic liquid medium could largely contribute to the formation of the pure single-crystalline gold dendrites under a kinetically controlled condition that is far from equilibrium. While plate-like gold structures were obtained in an aqueous solution without surfactants under a kinetically controlled synthesis,[61] gold nanoplates were prepared by photochemical reduction in the ionic liquid 1-butyl-3- methylimidazolium tetrafluoroborate ([BMIM][BF_4]) without any additional capping agent,[64] indicating that the ionic liquid may also drive the reaction into a kinetically controlled regime. It is interesting to note that 5-arm-star-shaped gold nanocrystals bounded with (331) and vicinal high-index facets were obtained in a deep eutectic solvent (DES), which is a kind of choline based ionic liquid.[13] It can be reasonably speculated that the DES could have also played a role in slowing down the reaction, leading to a kinetically controlled synthesis.

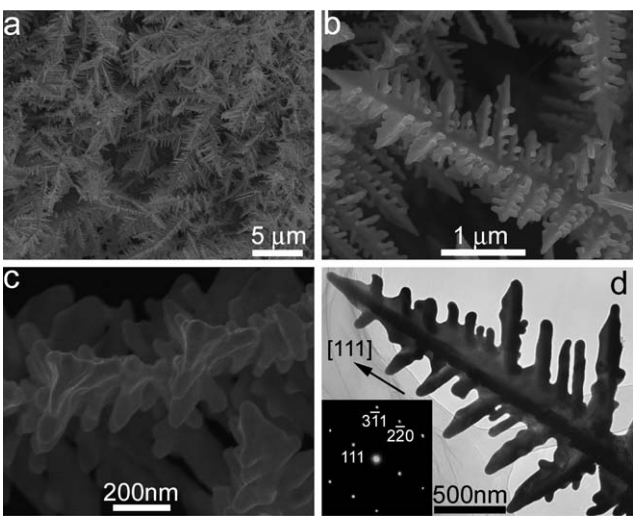

Fig. 5 SEM (a-c) and TEM (d) images of 3-fold symmetric gold dendrites grown in [BMIM][PF_6]. Inset shows the ED pattern corresponding to the whole area of the related image. Reprinted with permission from ref. 38, copyright 2008 American Chemical Society.

3. Single surfactant-directed synthesis

Among the various surfactants employed for the shape-controlled synthesis of gold nanocrystals, quaternary ammonium salt cationic surfactants are the most frequently used. As a typical cationic surfactant, CTAB has turned out to be very effective in the shape-controlled synthesis of gold nanorods. There have been a number of investigations on the effects of hydrophobic chains, headgroups, counterions, and impurity ions of cationic surfactants on the synthesis of gold nanocrystals. It was observed that the length of the hydrophobic chain in alkyltrimethylammonium bromides (C_nTAB) considerably influenced the morphology of the final gold nanostructures. The aspect ratio of the resulting gold nanoparticles increased from 1 to 23 as the length of the alkyl chain increased from decyl (C_{10}) to hexadecyl (C_{16}).[65] In the proposed "zipping" mechanism, gold nanorods were formed by the selective adsorption of the surfactant bilayer on the gold surface, resulting in van der Waals stabilization due to the interchain packing. The longer the tail length, the more stable the bilayer, and thus longer nanorods were produced. The existence of a bilayer, as opposed to a monolayer, is widely accepted and has been supported experimentally with IR spectroscopy, thermogravimetric analysis, and zeta potential analysis.[66] The surfactant bilayer consists of two surfactant leaflets; one is associated with the gold surface *via* the quaternary ammonium head groups, and the other has the surfactant head groups facing the aqueous media. This bilayer assembly is energetically favored as it guarantees hydrophobic interactions between the surfactant tails in the bilayer core and hydrophilic interactions of the charged head group with the aqueous media at the nanoparticle–solvent interface.

The headgroup of cationic surfactants also considerably influenced the morphology of the synthesized gold nanorods. For instance, a series of cationic surfactants with different headgroups, *i.e.* cetyltriethylammonium bromide (CTEAB), cetyltripropylammonium bromide (CTPAB), and cetyltributylammonium bromide (CTBAB), were used in seed-mediated syntheses of high-aspect-ratio gold nanorods in the presence of Ag^+ ions.[67] It was revealed that the average aspect ratio of the Au nanorods increased and the nanorod growth rate decreased as the cationic surfactant headgroup became larger, which could be attributed to the more stable bilayers formed on the Au surface from the surfactants with larger headgroups.

When an appropriate quantity of the Au seed solution was added into to the aqueous growth solutions containing desired quantities of CTAB, $HAuCl_4$, ascorbic acid (AA), and in some cases a small quantity of $AgNO_3$, a number of gold nanostructures, from rod-, rectangle-, hexagon-, cube-, triangle-, and

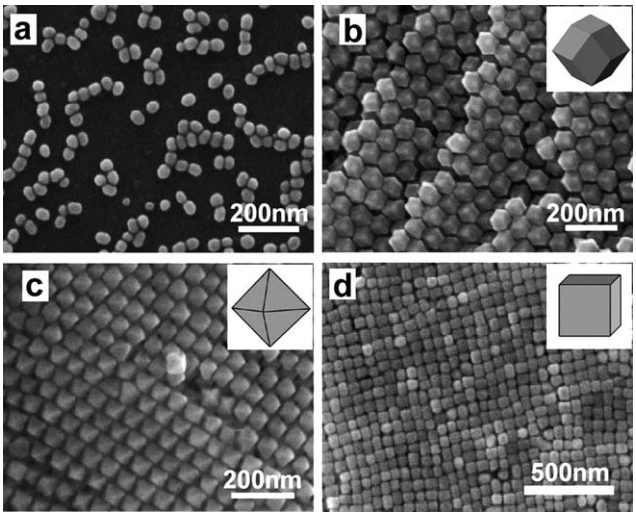

Fig. 6 SEM images of CPC-capped gold seeds (a), rhombic dodecahedral gold nanocrystals (b), octahedral gold nanocrystals (c), and cubic gold nanocrystals (d). Reprinted with permission from ref. 69, copyright 2009 American Chemical Society.

starlike outlines to branched Au nanocrystals, were obtained in high yield at room temperature.[68] The morphology and dimension of the Au nanocrystals depend on the concentrations of the seed particles, CTAB, and the reactants (Au^{3+} and AA), indicating that the final shape was largely dependent on the complex growth kinetic processes. However, it remained a challenge to selectively monodisperse, single-crystalline gold polyhedra bound by adjustable facets in large numbers. Recently, Tang and Xu and co-workers reported a versatile seed-mediated growth method for selectively synthesizing single-crystalline rhombic dodecahedral, octahedral, and cubic gold nanocrystals by using cetylpyridinium chloride (CPC) as the surfactant and CPC-capped single-crystalline gold nanocrystals as seeds (Fig. 6).[69] The CPC-capped gold seeds had a single-crystal nature and a relatively large size (~41.3 nm), which can avoid twinning during the growth process. CPC molecules were found to alter the surface energies of gold facets in the order {100} > {110} > {111} under the growth conditions, whereas the growth kinetics lead to the formation of thermodynamically less favored shapes. Octahedral nanocrystals bound by the {111} facets were formed when the capping of CPC on {111} facets dominates, while rhombic dodecahedral nanocrystals bound by the {110} facets were formed when the reduction of $AuCl^{4-}$ on the {111} facets dominates. Cubic gold nanocrystals bound by the {100} facets are formed by the introduction of bromide ions in the presence of CPC due to the cooperative work of cetylpyridinium and bromide ions. Interestingly, the obtained polyhedral gold nanocrystals can be easily assembled into highly ordered assemblies owing to the monodispersity of the polyhedra, as shown in Fig. 6.

Until recently, most synthetic methods involving CTAB have yielded gold polyhedra with convex shapes enclosed by low-index {111}, {100}, and/or {110} facets. Some recent efforts have been devoted to the synthesis of gold nanocrystals with high-index facets because these nanocrystals generally exhibit higher catalytic activities than those with only low-index facets due to the high densities of atomic steps exposed on the high-index facets. It is noteworthy that if CTAC (cetyltrimethylammonium chloride) was employed instead of CTAB, trisoctahedral gold nanocrystals enclosed by 24 high-index facets (*e.g.* {221} planes), which adopted a morphology of a concave cube, were produced by reducing $HAuCl_4$ with AA in the absence of Ag^+ ions.[46,49] In contrast, elongated tetrahexahedral (THH) gold nanocrystals enclosed by 24 {037} facets were successfully prepared in high yield *via* seed-mediated growth in CTAB solution in the presence of Ag^+ ions.[47] Interestingly, concave gold nanocubes enclosed by 24 high-index {720} facets were prepared in a monodisperse fashion by a similar seed-mediated synthetic method under identical synthesis conditions, except for the replacement of CTAB with CTAC (Fig. 7).[48] This result demonstrated that a simple change of the halide counterion in the surfactant induced a dramatic change in the product morphology and yielded a concave rather than convex cubic structure. However, the inherent mechanism remains unclear and further efforts aimed at understanding the role of the halide in the particle growth pathway are required. It may be noted that trace amounts of I^- ions could significantly influence the seed-mediated growth of anisotropic gold nanocrystals, and simple variation in the iodide concentration could result in a shape change of gold nanocrystals from pseudospherical nanoparticles to nanorods and nanoprisms.[70]

Besides cationic surfactants, other types of surfactants have also been used for synthesizing shape-controlled gold nanocrystals. For example, well-defined, dispersed, tadpole-shaped gold nanoparticles were synthesized by the reduction of $HAuCl_4$ with tri-sodium citrate in the presence of an anionic surfactant sodium dodecyl sulfonate. (SDSn).[71] Four different kinds of surfactants including CTAB, dodecyl sulfate (SDS), *N*-dodecyl-*N*,*N*-dimethyl-3-ammonio-1-propanesulfonate, a zwitterionic surfactant, and Tween-80, a nonionic surfactant, were used for the synthesis of gold nanostructures under the same experimental conditions, leading to the formation of multiple anisotropic nanostructures, such as rugged, leaf-like, dendritic, and tadpole-shaped gold nanocrystals,[72a] whereas another zwitterionic surfactant laurylsulfobetaine was employed for the synthesis of asymmetric branched gold nanoparticles with tunable near-infrared LSPR.[72b]

A universal approach for a high yield synthesis of nanoflowers of Au, Pt, and Pd was developed using an amino acid based surfactant, sodium *N*-(4-n-dodecyloxybenzoyl)-L-isoleucinate (SDBIL).[73] In particular, Au nanoflowers were formed in an acidic pH range (4.5–6.0), whereas spherical particles were

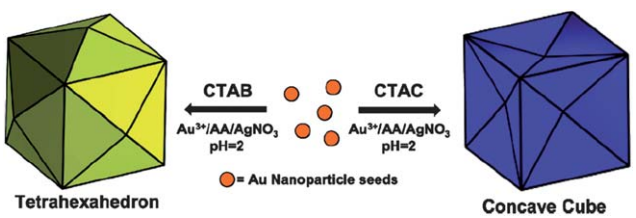

Fig. 7 Schematic illustration showing the effect of the counterion on the seed-mediated synthesis of gold nanocrystals with high-index facets: CTAC leads to the formation of concave cubes, and CTAB leads to the formation of tetrahexahedra (convex cubes). Reprinted with permission from ref. 48, copyright 2010 American Chemical Society.

formed in the alkaline pH range (7.0–8.5). The pH dependence of nanoflower formation can be explained by considering the self-assembly behavior of SDBIL. The surfactant SDBIL has a tendency to slowly form long fibrous aggregates in acidic pH; therefore, SDBIL can direct metal ions to deposit onto the surface of the seeds in an anisotropic manner, forming branches. In an alkaline pH, SDBIL self-assembles into spherical vesicles and thus does not lead to anisotropic growth of the seeds. In contrast, Liu *et al.* developed an effective approach to generate gold nanoflowers by vesicles made from a series of gemini amphiphiles with cationic headgroups and different spacer lengths.[74a] Jiang *et al.* employed a single tree-type multiple-head surfactant, bis(amidoethyl-carbamoylethyl) octadecylamine (C18N3) as both the reducing and capping agent for fabricating gold nano- and microplates.[74b] Gold decahedra and triangular plates were grown by a green one-step synthesis process in the presence of citric acid and the amphiphilic copolymer Tetronic T904.[75] Fine shape-control of gold nanoparticles was achieved in the presence of an amphiphilic polythiophene with an isothiouronium pendant, leading to the formation of p-conjugated polythiophene-capped Au nanoplates and nanocubes.[76] In addition, oleylamine was employed as the surfactant to direct the seed-mediated synthesis of ultrathin gold nanowires in toluene.[55]

4. Mixed surfactant-directed synthesis

In most cases, single surfactants have been employed as single capping agents for the controlled synthesis of gold nanocrystals. However, a mixture of two different surfactants can play special roles in crystal nucleation and growth of gold nanocrystals owing to the synergistic interactions of the binary surfactants with metal ions, as well as specific crystal planes. Therefore, mixed surfactants have also been used as binary capping agents for the shape-controlled synthesis of gold nanocrystals. In the original seed-mediated synthesis of gold nanorods using CTAB-capped seeds, gold nanorods with aspect ratios ranging from 1.5 to 4.5 were obtained when CTAB was used as the single surfactant in the growth solution.[20] When a binary surfactant mixture composed of benzyldimethylhexadecylammonium chloride (BDAC) and CTAB was used, longer nanorods with aspect ratios ranging from 4.6 to 10 were obtained, indicating the advantages of mixed surfactants in adjusting the aspect ratio of gold nanorods.

Mixed cationic/anionic surfactants represent an interesting mixed surfactant system. Earlier studies have shown that this system is very useful in the shape control of PbS nanocrystals.[77] Therefore, we explored the shape-controlled synthesis of gold nanocrystals using mixed cationic/anionic surfactants as binary capping agents. Single-crystalline gold nanobelts and unique gold nanocombs were successfully synthesized by the reduction of $HAuCl_4$ with ascorbic acid in aqueous solutions of the cationic surfactant CTAB and the anionic surfactant SDSn.[24] When the synthesis was conducted at 4 °C, gold nanobelts about 15–20 nm in thickness and ranging from 40 to 150 nm in width, which are single crystals elongated grown along the <110> direction with the top surface of the {111} plane, were obtained (Fig. 8a,b). In contrast, when the synthesis was conducted at 27 °C, gold nanobelts about 20–30 nm in thickness and ranging from 40 to 200 nm in width, which are single crystals grown along the [211] direction with the (111) plane as the top surface, were produced (Fig. 8c,d). Fig. 8e presents a schematic illustration of the growth direction of the <110>-oriented gold nanobelts obtained at 4 °C and the <211>-oriented gold nanobelts obtained at 27 °C, where a {111}-oriented hexagonal plate exhibiting 6 equivalent {110} planes is drawn to clearly show the relative angles between different planes and growth direction. The CTAB-SDSn mixture could strongly adsorb on the {111} planes of cubic gold at both temperatures; meanwhile, it could less strongly adsorb on the {211} surfaces at 4 °C and on the {110} surfaces at 27 °C due to some cooperative effects of the binary surfactants, leading to the formation of <110>-oriented nanobelts and <211>-oriented nanobelts at 4 °C and 27 °C, respectively.

When the reaction solution was initially kept at 4 °C for 0.5 h and subsequently let to stand at 27 °C for 12 h, unique gold nanocombs made of nanobelts of about 20–30 nm in thickness could be obtained in addition to nested Au nanobelts (Fig. 9a,b). The obtained comb-like nanostructures normally consist of a stem belt and numerous lateral belts grown perpendicularly on one side of the stem. The ED pattern of a single nanocomb suggests that the gold nanocomb is actually a single crystal with the stem nanobelt grown along the <110> direction and the side nanobelts grown along the <211> direction, which are consistent with the growth directions of Au nanobelts grown at 4 and 27 °C, respectively. A tentative growth mechanism for the gold

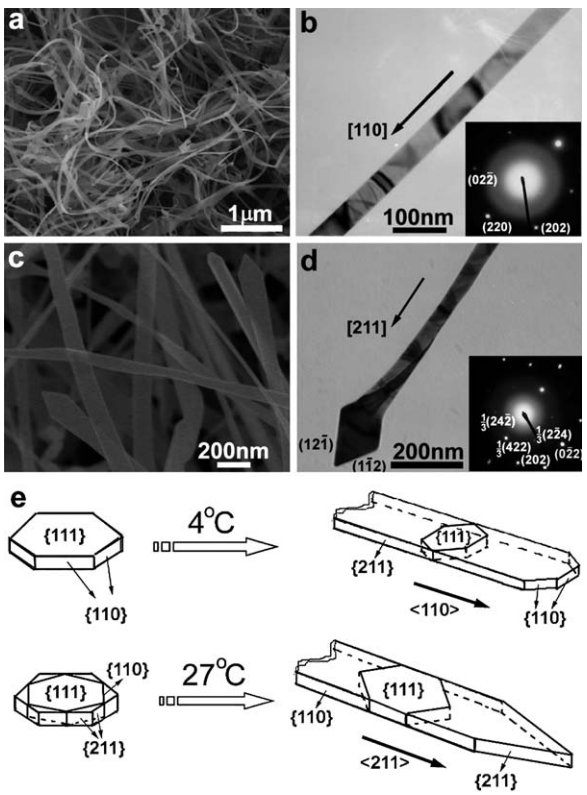

Fig. 8 SEM (a,c) and TEM (b,d) images of gold nanobelts obtained in a mixed CTAB-SDSn solution at 4 °C (a,b) and 27 °C (c,d). (e) Schematic illustration showing the crystal growth direction of the nanobelts. Reprinted with permission from ref. 24, copyright 2008 American Chemical Society.

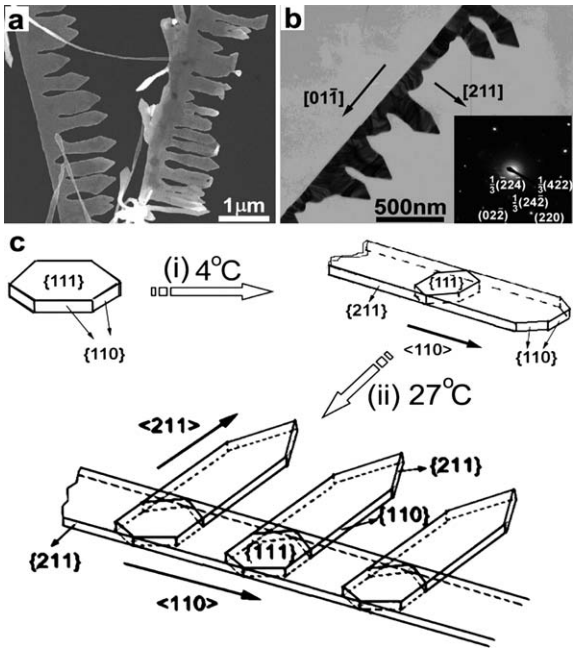

Fig. 9 SEM (a) and TEM (b) images of gold nanocombs obtained in a mixed CTAB-SDSn solution by two-step growth. (c) Schematic illustration showing the crystal growth direction of the nanocombs. Reprinted with permission from ref. 24, copyright 2008 American Chemical Society.

nanocombs is illustrated in Fig. 9c. The growth of gold nanocombs *via* a two-step process with temperature changing from 4 °C to 27 °C could be rationalized by considering that the <110>-oriented stem nanobelts formed at 4 °C initially, which was followed by the gradual growth of <211>-oriented lateral nanobelts on one side of the stem. The reason why the lateral nanobelts of the nanocombs just grow along one side remains unclear, but it may be related to the kinetically controlled growth process. Such a breaking of symmetry in the crystal growth represents an interesting topic worthy of further study.[61] It should be noted that the yield of the nanocomb structures is still not high (usually less than 10%) and further efforts are needed to optimize the synthesis conditions to realize a high-yield synthesis.

It is interesting to note that ultrathin gold nanowires with a diameter of 9 nm were synthesized by the reduction of $HAuCl_4$ in a mixture of oleylamine and oleic acid, which may be approximately considered as another mixed cationic/anionic surfactant system.[78] The obtained ultrathin single-crystalline gold nanowires show good electron conductivity and can be used as a molecular-scale interconnect for nanoelectronic applications. In addition, there have been numerous examples involving other systems of mixtures of different surfactants, as well as mixtures of one surfactant with other capping agents. One-step green synthesis of gold nanostructures (*e.g.* prisms and hexagonal structures) was achieved using naturally occurring biodegradable plant surfactants, which are mixtures of natural surfactants.[79] High-yield synthesis of tetrahedral-like gold nanotripods were produced in an aqueous mixture of CTAB and hexamethylenetetramine (HMT).[80] Recently, highly thin, electron-transparent gold nanoplates were obtained in a ternary mixtures of CTAB, poly(vinyl pyrrolidone) (PVP), and poly(ethylene glycol) (PEG).[81] Hence the simultaneous utilization of two or more capping agents may represent a useful strategy in the shape control of gold nanocrystals.

5. Supramolecular surfactant-directed synthesis

Since the structure of a surfactant plays a significant role in determining the shape of gold nanocrystals, it is expected that the nanocrystal morphology can be readily tuned if one can find a way to adjust rationally the surfactant structure used in nanocrystal synthesis. Fortunately, this goal can be partly realized through supramolecular assembly of a surfactant with a host molecule to form a supramolecular surfactant. As a class of water-soluble and nontoxic cyclic oligosaccharides with a hydrophilic exterior and a hydrophobic interior, cyclodextrins (CDs) have been extensively investigated in host–guest chemistry for construction of versatile supramolecular complexes owing to their special hydrophobic cavities.[82] In particular, CDs can form supramolecular complexes with surfactants carrying hydrophobic chains *via* the host–guest interaction,[83] which may be considered as supramolecular amphiphiles,[84] or supramolecular surfactants. The thus-formed supramolecular surfactant may exert a subtle control on the growth of Au nanocrystals in solution due to the special adsorption behaviors of the supramolecular complexes, thereby leading to a delicate control over the nanocrystal morphology.

As the first example of supramolecular surfactant-directed synthesis of gold nanocrystals, we synthesized well-defined planar gold dendrites by reducing chloroauric acid in aqueous mixed solutions of dodecyltrimethylammonium bromide (DTAB) and β-CD (Fig. 10).[39] The typical product consists almost entirely of hyperbranched dendritic structures up to ~2 μm in length (Fig. 10a). Each dendrite has a planar, highly symmetrical structure, which consists of a pronounced trunk with two groups of symmetrical side branches grown on the trunk with an angle of ~60° (Fig. 10b,c). The related electron

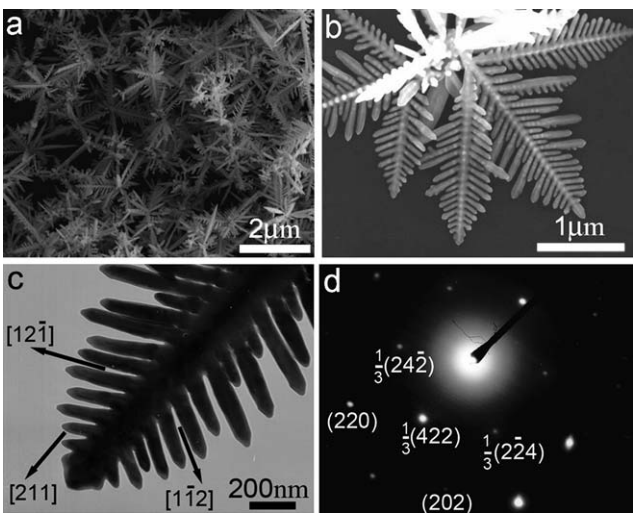

Fig. 10 SEM images (a,b), TEM image (c), and ED pattern (d) of planar gold nanodendrites grown in mixed DTAB/β-CD solution. Reprinted with permission from ref. 39, copyright 2010 American Chemical Society.

diffraction (ED) pattern of the whole dendrite, shown in Fig. 10d, suggests that the whole Au dendrite is a planar single crystal with the (111) plane as the top surface, and both the trunk and the side branches are grown along the <211> direction. It was revealed that the formation of the DTAB-β-CD supramolecular surfactant due to host–guest interaction is indispensable for the fabrication of these unique planar Au nanodendrites, which could be ascribed to the special binding behaviors of the supramolecular surfactant. Moreover, it was found that the nanocrystal shape was largely determined by the CD-to-DTAB molar ratio and a variety of Au nanostructures, such as branched particles consisting of rodlike branches and flowerlike particles consisting of platelike petals, could be readily obtained by simply changing the CD-to-DTAB molar ratio.

Based on the experimental results, a tentative growth mechanism for the gold nanostructures obtained at various molar ratios of CD-to-DTAB is illustrated in Fig. 11. Irregular particles exhibiting faceted surfaces were the predominant product in the absence of β-CD. Upon the addition of β-CD, the 1 : 1 inclusion complex would easily form between DTAB and β-CD *via* the host–guest interaction, and the formed DTAB-β-CD supramolecular surfactant would replace some of the DTAB molecules. At a CD-to-DTAB molar ratio of 0.3, branched particles were obtained, which could be ascribed to the weaker protection of the mixed adsorption film of the DTAB molecules and the supramolecular surfactant. If the CD-to-DTAB molar ratio was increased to 0.5, more DTAB molecules on the Au crystal surfaces were replaced by the supramolecular surfactant, favoring the formation of the unique planar Au dendrites under nonequilibrium conditions. On further increasing the CD-to-DTAB molar ratio to 2, flowerlike particles consisting of platelike petals became the predominant product, which could be partially ascribed to the more effective capping of β-CD molecules to prevent further growth of Au crystals due to the high concentration of free β-CD in solution. Nevertheless, a detailed investigation of the interaction between the supramolecular surfactant and gold crystals is needed to fully elucidate the growth mechanism of the unique Au nanodendrites.

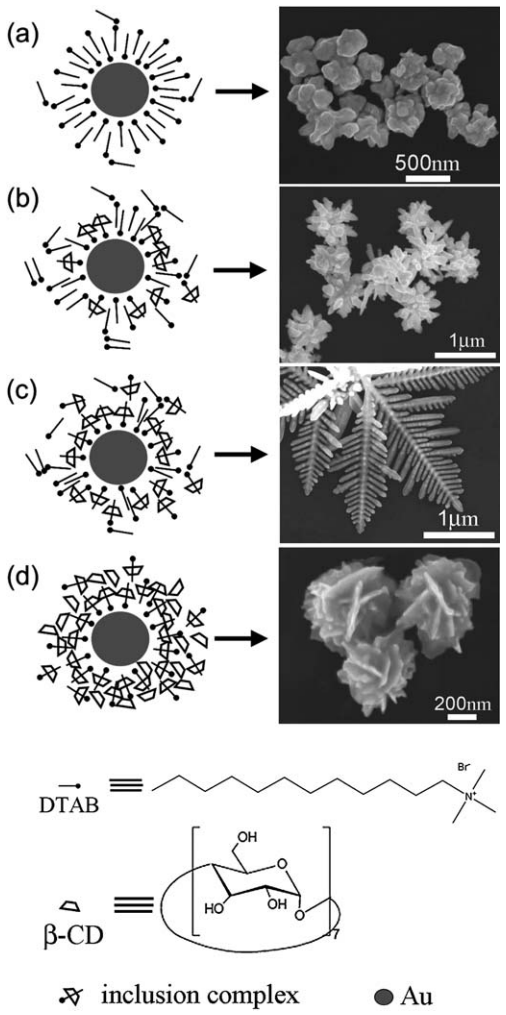

Fig. 11 Schematic illustration of the possible formation mechanism of gold nanostructures obtained in a mixed DTAB/β-CD solution. [β-CD]/[DTAB]: (a) 0; (b) 0.3; (c) 0.5; (d) 2. Reprinted with permission from ref. 39, copyright 2010 American Chemical Society.

6. Metal–surfactant complex-templated synthesis

Templating synthesis is a powerful method for the controlled synthesis of shaped nanocrystals; however, the available templates for colloidal synthesis of gold nanocrystals are still rather limited. In the classical seed-mediated synthesis of gold nanorods in the presence of CTAB, originally it was thought that the rodlike micelles formed by CTAB in aqueous solution would play the role of soft templates,[19] but later on a more reasonable mechanism based on the preferential binding of CTAB to certain crystal faces of gold nanorods was put forward and became widely accepted.[53] It is worthwhile to search for other feasible colloidal templates for the shape-controlled synthesis of gold nanocrystals. In this regard, metal–surfactant complexes with desirable morphologies, which are formed by Au^{I} or Au^{III} and surfactants through binding interactions (*e.g.* aurophilic attraction and electrostatic combination), can be employed as reactive sacrificial templates for the shape-controlled synthesis of gold nanocrystals.

Xia and co-workers reported a facile method for preparing ultrathin Au nanowires using [(oleylamine)AuCl] complex chains formed through aurophilic attraction.[85] The aurophilic bonding of organometallic complexes formed from AuCl and oleylamine can lead to the formation of 1D polymeric chains. Because of interactions such as van der Waals attraction between the side chains, the 1D structure can form polymeric strands with backbones of Au^{I} ions surrounded by alkyl ligands. When the Au^{I} is converted to Au^{0} under slow reduction, the nucleation and growth of Au can be mediated by the 1D polymer strands to generate ultrathin nanowires (Fig. 12). The product was primarily composed of [111]-oriented ultrathin gold nanowires with an average diameter of 1.8 nm and an estimated yield of ~70%.

Recently, we reported a facile, high-yield synthesis of unique porous gold nanobelts by morphology-preserved transformation from metal–surfactant complex precursor nanobelts formed by $HAuCl_4$ and $Br^{-}[(CH_3)_3N^{+}–(CH_2)_{12}–N^{+}(CH_3)_3]Br^{-}$ ($N\text{-}C_{12}\text{–}NBr_2$), a bolaform surfactant containing two quaternary ammonium headgroups.[86] Fig. 13 shows typical SEM and TEM

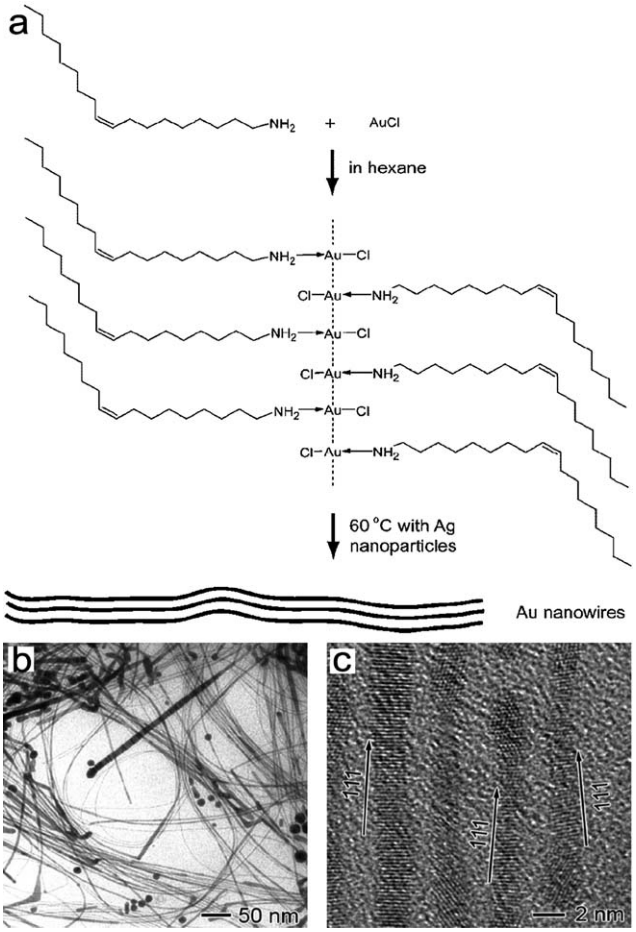

Fig. 12 (a) Schematic illustration of the ultrathin Au nanowire formation from a chain-like oleylamine–AuCl complex template. TEM (b) and HRTEM (c) images of the ultrathin Au nanowires. Reprinted with permission from ref. 85, copyright 2008 American Chemical Society.

images of the porous gold nanobelts obtained by adding $NaBH_4$ to a solution containing 0.25 mM N–C_{12}–NBr_2 and 0.2 mM $HAuCl_4$. It can be seen that the product consists of curled, porous gold nanobelts with a thickness of about 10–20 nm, and width about 100–200 nm. Such porous gold nanobelts combine the advantages of both 1D structures and nanoporous structures, and may be an appealing material in application areas including catalysis.

Further study showed that curled nanobelts of ~500 nm in width and 50–100 nm in thickness appeared soon after mixing N–C_{12}–NBr_2 and $HAuCl_4$ in solution without $NaBH_4$. Accordingly, the formation process of the porous gold nanobelts is tentatively proposed as follows (Fig. 14): When N–C_{12}–NBr_2 was mixed with $HAuCl_4$, a stoichiometric N–C_{12}–$N(AuCl_4)_2$ complex formed immediately *via* electrostatic interaction as well as van der Waals interaction between the positively charged headgroups and the negatively charged $AuCl_4^-$ ions, which quickly self-assembled and crystallized into curled nanobelts. As the reductant $NaBH_4$ was added, the N–C_{12}–$N(AuCl_4)_2$ complex was reduced to gold nanocrystals, resulting in the formation of porous gold nanobelts with shrunken sizes.

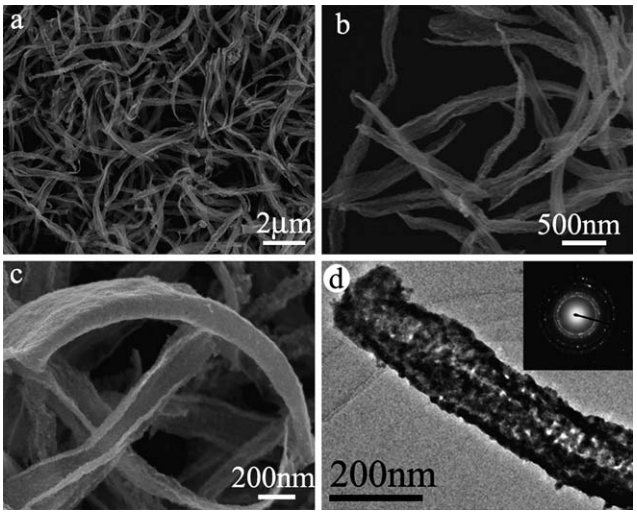

Fig. 13 SEM (a–c) and TEM (d) images of porous gold nanobelts obtained from belt-like N–C_{12}–$N(AuCl_4)_2$ complex template. Reprinted with permission from ref. 86, copyright 2010 American Chemical Society.

7. Applications of shape-controlled gold nanocrystals

While the morphology control of gold nanocrystals is developing rapidly, the applications of shape-controlled gold nanocrystals are keeping up with it. Shaped gold nanocrystals may find promising applications in a wide range of technologically important areas including catalysis, sensing, biological and

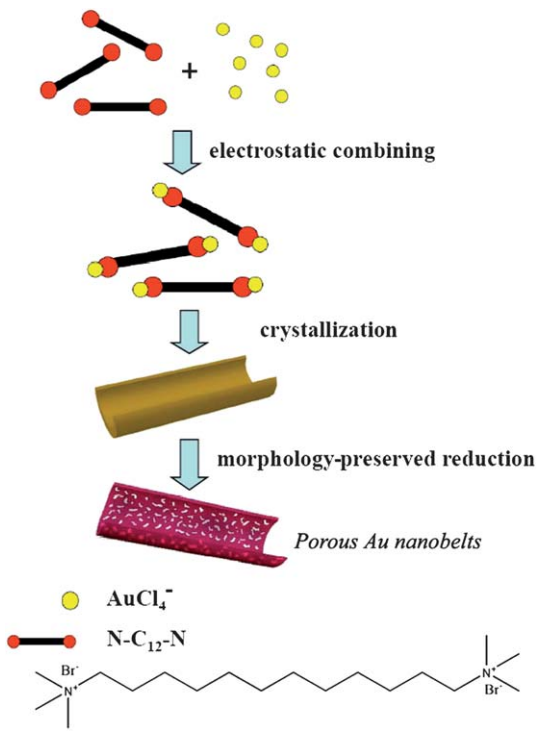

Fig. 14 Schematic illustration of the formation mechanism of porous gold nanobelts *via* an N–C_{12}–$N(AuCl_4)_2$ complex template. Reprinted with permission from ref. 86, copyright 2010 American Chemical Society.

biomedical applications, as well as electronic, photonic and plasmonic applications. In particular, gold nanorods have shown a great potential in biological and biomedical applications including biosensing, bioimaging, photothermal therapy, gene and drug delivery, and tissue repair.[4,43,87,88] Considering that there have been a number of exhaustive reviews concerning the applications of gold nanocrystals in biological and biomedical applications,[2–6,10–12] here we will just focus on the applications of shape-controlled gold nanocrystals in catalysis and molecular sensing including SPR-based and SERS-based sensing.

7.1 Catalysis

Gold nanocrystals are attractive for use as nanoscale catalysts because of their nontoxic nature, high surface-to-volume ratio, and the ability to catalyze a variety of chemical reactions such as hydrogenation, CO oxidation, selective oxidation, and nucleophilic additions.[9,89] Both the reactivity and selectivity of a nanocrystal catalyst can be tailored by controlling the shape of the nanocrystal because the shape determines the exposed facets and the number of atoms located at the edges or corners.[17] Generally, gold nanocrystals with more active sites, which are associated with crystal defects including edges and corners, and with highly active facets, which are associated with high-index facets, tend to exhibit improved catalytic performance.

The application of shaped gold nanocrystals in electrocatalysis has been explored. For example, the current–potential curves of electrocatalytic reduction of H_2O_2 on different Au electrodes are compared in Fig. 15. The star-shaped gold nanoparticles bounded with (331) and vicinal high-index facets exhibit the highest catalytic activity among the investigated Au electrodes, which is reflected by the significantly positive shift of the onset potential for H_2O_2 reduction and the largest reduction current density per unit Au surface area. The high catalytic activity of the star-shaped nanoparticles towards H_2O_2 electrocatalytic reduction can be attributed to their high-index facets, which provide a high density of stepped atoms. Similarly, dendritic gold nanostructures exhibited nice catalytic activity toward the electrochemical methanol oxidation[38,39] and electrochemical oxygen reduction. The observed high electrocatalytic activity could be related to the presence of more defects and more high-index facets in the gold nanodendrites.[40] Similarly, trisoctahedral gold nanocrystals enclosed by 24 high-index facets, such as {221} planes, showed considerably higher electrocatalytic activity than a normal polycrystalline gold electrode, confirming that high-index facets exhibit improved catalytic performance due to the presence of high-density atomic steps, ledges, kinks, and dangling bonds.[46]

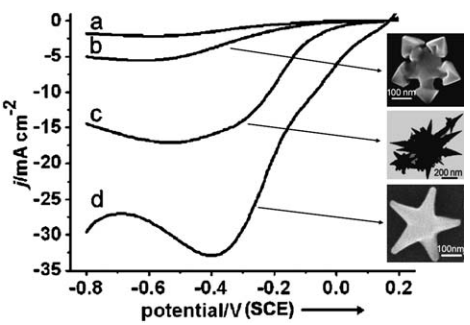

Fig. 15 Current–potential curves of the electrocatalytic reduction of 20 mM H_2O_2 in 0.1 M phosphate-buffered solution at a scan rate of 50 mV s^{-1}: (a) polycrystalline Au electrode, (b) snowflake-like Au nanoparticles, (c) nanothorns, (d) star-shaped Au nanoparticles. Insets shows SEM images of the shaped Au NPs. Reprinted with permission from ref. 13, copyright 2008 Wiley-VCH Verlag GmbH & Co.

While spherical Au nanoparticles exhibited essentially no catalytic activity toward the Suzuki–Miyaura coupling reaction of phenyl boronic acid and iodobenzene in water, Au nanoflowers with high-index facets were able to catalyze the reaction, although the yield was low (5%).[73] The superior catalytic activity of the Au nanoflowers over spherical nanoparticles may be ascribed to the exposed high-index facets that result in more catalytically active Au atoms on edges or corners. On the other hand, the reduction of *p*-nitrophenol by $NaBH_4$ in solution has also been used as a model reaction to investigate the catalytic properties of gold nanocrystals with different morphologies. A comparison study of the catalytic properties of Au-based nanocages, nanoboxes, and nanoparticles was carried out.[90] The obtained kinetic data indicate that the Au-based nanocages are catalytically more active than both the nanoboxes and nanoparticles, probably due to their extremely thin but electrically continuous walls, the high content of Au, and the accessibility of both inner and outer surfaces through the pores in the walls. A comparison study of the catalytic properties of solid gold nanobelts and porous gold nanobelts was also carried out, which shows that the porous gold nanobelts exhibit enhanced catalytic activity owing to their porous structures.[86]

It may be noted that there have been rare reports on the application of shaped gold nanocrystals in gas-phase catalysis, although the electrochemical and chemical catalysis of gold nanocrystals with varied morphologies in solution phase has been frequently reported. This phenomenon may be rationalized by considering that most of the obtained well-defined gold nanocrystals enclosed by high-index facets have relatively large sizes (typically larger than 10 nm), while gold nanocatalysts used in gas-phase catalysis usually require very small particle sizes (<5 nm) since larger gold nanocrystals generally exhibit rather low catalytic activity. Recent theoretical calculations have shown that particle morphology is a key factor in influencing oxygen activation on gold nanoparticles, and hence their catalytic performance in gas-phase reactions.[91] It would be highly desirable to realize the high-yield synthesis of shaped gold nanocrystals with smaller sizes for investigating the relationship between the shape and the catalytic activity of gold nanocrystals in gas-phase reactions. On the other hand, it is worth noting that the stability of gold nanocrystals is an important character for evaluating their catalytic performance. Extensive studies have shown that the shape of a metal nanocrystal can change in response to variations in temperature and the surrounding environment; particularly, it has been shown that the morphology of gold nanoparticles may be altered by CO adsorption.[92] Obviously, the issue regarding the stability of gold nanocatalysts needs to be addressed to practically implement the shape-controlled nanocrystals as industrial catalysts.

7.2 Molecular sensing

Shaped gold nanocrystals can be used for molecular sensing based on either surface plasmon resonance (SPR) or surface-enhanced Raman spectroscopy (SERS). It is known that the SPR wavelength of gold nanocrystals depends on the dielectric constant of the surrounding medium, which provides a great opportunity to monitor the changes of the local environment of the nanocrystals, and thus they can be used for sensing.[43] The sensitivity is largely dependent on the shape of the nanocrystals, and anisotropic nanocrystals normally give higher sensitivity than spherical nanoparticles. For example, gold nanorods are highly suited for SPR-based sensing and multiplex biosensor assays which use the different responses of gold nanorods to different targets. This has already been demonstrated.[93] Recently, it has been found that gold nanoframes have sensitivity factors that are 12, 7, and 3 times higher than those of gold nanospheres, gold nanocubes, and gold nanorods, respectively, which may be ascribed to the coupling between their interior and exterior surface fields.[94] Fig. 16a shows the SPR spectra of 42 nm Au nanoframes with a wall thickness of 9 nm assembled as monolayers and measured in different media. The SPR of all the four Au nanoframes with different aspect ratios red-shifts as the refractive index of the solvent increases linearly, and the sensitivity factors increase as the aspect ratios increase (Fig. 16b). These nanoframes are excellent nanosensors in the near-infrared region with the strongest plasmonic fields and largest sensitivity factors of any single nanoparticles known.

Owing to its high sensitivity and chemical specificity, SERS has been demonstrated as a powerful spectroscopic technique for low-level detection and analysis. Covering a substrate with nonspherical gold nanocrystals is an efficient way to enhance the Raman scattering since intense near-field enhancement is localized around sharp vertices. In this regard, gold nanostructures with sharp tips, corners or edges are promising SERS substrates for the sensitive detection of the probe molecules. Particularly, branched gold nanocrystals with tips, such as stars, flowers, and dendrites, are attracting increasing interest for application in SERS.[34–42,52] For instance, gold nanocombs,[24] nanodendrites,[39] and nanowires covered with sharp tips[52] exhibit high SERS activities. Through systematically adjusting the size, morphology, and monodispersity of Au nanostars, the importance of sharp tips on the enhancing behavior of these nanoparticles in SERS was confirmed.[35] The high degree of SERS activity of gold mesoflowers enabled the SERS-based imaging of a single mesoflower.[36] It is noteworthy that a multifunctional gold nano-popcorn-based SERS assay for targeted sensing, nanotherapy treatment, and in situ monitoring of photothermal nanotherapy response has been reported recently.[95] This nanotechnology-driven assay could have enormous potential applications in rapid, on-site targeted diagnosis, nanotherapy treatment, and monitoring of the nanotherapy process, which are critical for providing effective treatment of cancer.

8. Summary and outlook

Surfactants have been widely used in the shape-controlled synthesis of gold nanocrystals, where they play multiple key roles through various mechanisms associated with the general strategies in shape control. Firstly, surfactants can act as efficient adsorbates or capping agents to protect gold nanocrystals and direct their isotropic growth. Secondly, surfactants can significantly affect the formation of crystal seeds and the growth from seeds to final nanocrystals, thus controlling the nanocrystal shape in seed-mediated syntheses. Thirdly, surfactants can form ordered structures through either self-assembly in solution or co-assembly with inorganic species, which can serve as effective templates for tailoring the nanocrystal shape. Lastly, surfactants can strongly interact with the reacting species and the growing nanocrystals, and hence considerably influence the growth kinetics or the reaction regime, which would exert delicate control over the nanocrystal shape. In most cases, single surfactants are used as the capping agents in the shape-controlled synthesis of gold nanocrystals, and a variety of structural parameters including hydrophobic chains, headgroups, counterions, and impurity ions show considerable effects on the nanocrystal shape. Recently, there are some emerging

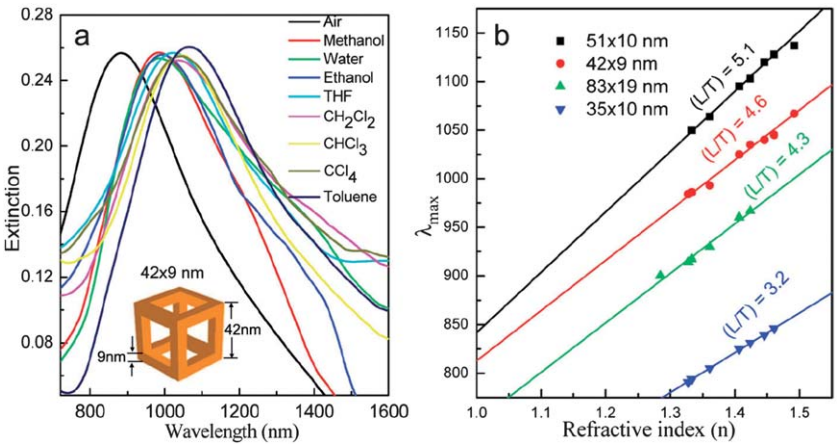

Fig. 16 (a) SPR of gold nanoframes (42 nm wall length and 9 nm wall thickness) monolayers assembled on the surface of quartz substrates and measured in different solvents. (b) Relationship between the refractive index and the SPR peak maximum of gold nanoframes with different aspect ratios. The sensitivity factors determined from the slope of each line for each aspect ratio are 620 ± 15, 516 ± 24, 508 ± 33, and 409 ± 6 for nanoframes of aspect ratios 5.1, 4.6, 4.3, and 3.2, respectively. Reprinted with permission from ref. 94, copyright 2010 American Chemical Society.

approaches towards shape control of gold nanocrystals involving the rational utilization of surfactants; examples include the use of mixed surfactants, supramolecular surfactants, and metal–surfactant complex templates. Currently, reliable, high-yield, colloidal synthesis of gold nanorods, triangular nanoprisms, and platonic polyhedra with the assistance of surfactants has been realized. There has been increasing interest in the surfactant-assisted synthesis of polyhedral gold nanocrystals exhibiting high-index facets, high-aspect-ratio 1D nanostructures with tailored structures, as well as branched gold nanocrystals, such as stars, flowers, combs, and dendrites.

Despite a great success in the surfactant-assisted synthesis of shape-controlled gold nanocrystals, some great challenges remain ahead in this research area. A more comprehensive understanding of the mechanisms involved in surfactant-engaged synthesis, and the development of general synthetic schemes for gold nanocrystals with desired shapes and structures, are of critical importance for the continued success and advancement of this field. Moreover, detailed investigation of the relationship between the property and the shape of gold nanocrystals is demanded for advancing the applications of the obtained colloidal gold nanocrystals. For industrial applications of shaped gold nanocrystals in catalysis, smaller gold nanocrystals showing high-index facets or with many active sites are desirable, and issues regarding catalyst stability and poisoning must be addressed; for applications in SERS-based molecular sensing, branched gold nanocrystals with more regular structures and the ordered arrangements of the shaped nanocrystals are essential to obtain reproducible and predictable SERS signals. In addition to the flourishing advances in the biological and biomedical applications of shaped gold nanocrystals, their applications in other technological areas still need to be explored. Actually, there have been some exciting examples worthy of attention; for example, five-dimensional optical recording was realized by exploiting the unique properties of the longitudinal SPR of gold nanorods,[96a] while light-driven nanoscale plasmonic motors were demonstrated by using planar gammadion gold nanostructures.[96b] Recently, unique DNA-nanoparticle superlattices were formed from a variety of anisotropic gold nanocrystals (*e.g.* nanorods, triangular nanoprisms, and rhombic dodecahedra), which may be used in plasmonic-based circuitry or waveguides.[97] It is noteworthy that shape-controlled gold nanocrystals may find wide potential applications, such as light concentration and manipulation,[98] photovoltaic devices,[99] and Fano resonance-related applications,[100] owing to their unique plasmonic properties.

Acknowledgements

Financial support from NSFC (Grants 20873002, 21073005, 20633010, and 50821061) and MOST (Grant 2007CB936201) is gratefully acknowledged.

References

1 S. Eustis and M. A. El-Sayed, *Chem. Soc. Rev.*, 2006, **35**, 209.
2 P. K. Jain, X. Huang, I. H. El-Sayed and M. A. El-Sayed, *Acc. Chem. Res.*, 2008, **41**, 1578.
3 C. J. Murphy, A. M. Gole, J. W. Stone, P. N. Sisco, A. M. Alkilany, E. C. Goldsmith and S. C. Baxter, *Acc. Chem. Res.*, 2008, **41**, 1721.
4 C. J. Murphy, A. M. Gole, S. E. Hunyadi, J. W. Stone, P. N. Sisco, A. Alkilany, B. E. Kinard and P. Hankins, *Chem. Commun.*, 2008, 544.
5 M. Hu, J. Chen, Z.-Y. Li, L. Au, G. V. Hartland, X. Li, M. Marquez and Y. Xia, *Chem. Soc. Rev.*, 2006, **35**, 1084.
6 C. M. Cobley, J. Chen, E. C. Cho, L. V. Wang and Y. Xia, *Chem. Soc. Rev.*, 2011, **40**, 44.
7 R. Sardar, A. M. Funston, P. Mulvaney and R. W. Murray, *Langmuir*, 2009, **25**, 13840.
8 S. K. Ghosh and T. Pal, *Chem. Rev.*, 2007, **107**, 4797.
9 A. S. K. Hashmi and G. J. Hutchings, *Angew. Chem., Int. Ed.*, 2006, **45**, 7896.
10 R. A. Sperling, P. R. Gil, F. Zhang, M. Zanella and W. J. Parak, *Chem. Soc. Rev.*, 2008, **37**, 1896.
11 E. Boisselier and D. Astruc, *Chem. Soc. Rev.*, 2009, **38**, 1759.
12 D. A. Giljohann, D. S. Seferos, W. L. Daniel, M. D. Massich, P. C. Patel and C. A. Mirkin, *Angew. Chem., Int. Ed.*, 2010, **49**, 3280.
13 H.-G. Liao, Y.-X. Jiang, Z.-Y. Zhou, S.-P. Chen and S.-G. Sun, *Angew. Chem., Int. Ed.*, 2008, **47**, 9100.
14 T. K. Sau, A. L. Rogach, F. Jackel, T. A. Klar and J. Feldmann, *Adv. Mater.*, 2010, **22**, 1805.
15 M. Grzelczak, J. Pérez-Juste, P. Mulvaney and L. M. Liz-Marzán, *Chem. Soc. Rev.*, 2008, **37**, 1783.
16 A. R. Tao, S. Habas and P. D. Yang, *Small*, 2008, **4**, 310.
17 Y. Xia, Y. Xiong, B. Lim and Sara E. Skrabalak, *Angew. Chem., Int. Ed.*, 2009, **48**, 60.
18 T. K. Sau and A. L. Rogach, *Adv. Mater.*, 2010, **22**, 1781.
19 N. R. Jana, L. Gearheart and C. J. Murphy, *Adv. Mater.*, 2001, **13**, 1389.
20 B. Nikoobakht and M. A. El-Sayed, *Chem. Mater.*, 2003, **15**, 1957.
21 C. Wang and S. Sun, *Chem. Asian J.*, 2009, **4**, 1028.
22 H. Feng, Y. Yang, Y. You, G. Li, J. Guo, T. Yu, Z. Shen, T. Wu and B. Xing, *Chem. Commun.*, 2009, 1984.
23 J. Zhang, J. Du, B. Han, Z. Liu, T. Jiang and Z. Zhang, *Angew. Chem., Int. Ed.*, 2006, **45**, 1116.
24 N. Zhao, Y. Wei, N. Sun, Q. Chen, J. Bai, L. Zhou, Y. Qin, M. Li and L. Qi, *Langmuir*, 2008, **24**, 991.
25 R. Jin, Y. Cao, C. A. Mirkin, K. L. Kelly, G. C. Schatz and J. G. Zheng, *Science*, 2001, **294**, 1901.
26 A. Miranda, E. Malheiro, E. Skiba, P. Quaresma, P. A. Carvalho, P. Eaton, B. de Castro, J. A. Shelnuttcd and E. Pereira, *Nanoscale*, 2010, **2**, 2209.
27 F. Kim, S. Connor, H. Song, T. Kuykendall and P. Yang, *Angew. Chem., Int. Ed.*, 2004, **43**, 3673.
28 D. Seo, C. I. Yoo, J. C. Park, S. M. Park, S. Ryu and H. Song, *Angew. Chem., Int. Ed.*, 2008, **47**, 763.
29 G. H. Jeong, M. Kim, Y. W. Lee, W. Choi, W. T. Oh, Q. H. Park and S. W. Han, *J. Am. Chem. Soc.*, 2009, **131**, 1672.
30 C. C. Li, K. L. Shuford, M. H. Chen, E. J. Lee and S. O. Cho, *ACS Nano*, 2008, **2**, 1760.
31 M. Yavuz, S. W. Li and Y. Xia, *Chem. Eur. J.*, 2009, **15**, 13181.
32 S. E. Skrabalak, J. Chen, Y. Sun, X. Lu, L. Au, C. M. Cobley and Y. Xia, *Acc. Chem. Res.*, 2008, **41**, 1587.
33 N. Zhao, L. Li, T. Huang and L. Qi, *Nanoscale*, 2010, **2**, 2418.
34 P. S. Kumar, I. Pastoriza-Santos, B. Rodriguez-Gonzalez, F. J. Garcia de Abajo and L. M. Liz-Marzan, *Nanotechnology*, 2008, **19**, 015606.
35 S. Barbosa, A. Agrawal, L. Rodríguez-Lorenzo, I. Pastoriza-Santos, R. A. Alvarez-Puebla, A. Kornowski, H. Weller and L. M. Liz-Maráan, *Langmuir*, 2010, **26**, 14943.
36 P. R. Sajanlal and T. Pradeep, *Nano Res.*, 2009, **2**, 306.
37 Z. Wang, J. Zhang, J. M. Ekman, P. J. A. Kenis and Y. Lu, *Nano Lett.*, 2010, **10**, 1886.
38 Y. Qin, Y. Song, N. Sun, N. Zhao, M. Li and L. Qi, *Chem. Mater.*, 2008, **20**, 3965.
39 T. Huang, F. Meng and L. Qi, *Langmuir*, 2010, **26**, 7582.
40 X. Xu, J. Jia, X. Yang and S. Dong, *Langmuir*, 2010, **26**, 7627.
41 W. Ye, J. Yan, Q. Ye and F. Zhou, *J. Phys. Chem. C*, 2010, **114**, 15617.
42 M. Pan, S. Xing, T. Sun, W. Zhou, M. Sindoro, H. H. Teo, Q. Yanb and H. Chen, *Chem. Commun.*, 2010, **46**, 7112.
43 X. Huang, S. Neretina and M. A. El-Sayed, *Adv. Mater.*, 2009, **21**, 4880.
44 V. Sharma, K. Park and M. Srinivasarao, *Mater. Sci. Eng., R*, 2009, **65**, 1.

45 J. E. Millstone, S. J. Hurst, G. S. Metraux, J. I. Cutler and C. A. Mirkin, *Small*, 2009, **5**, 646.
46 Y. Ma, Q. Kuang, Z. Jiang, Z. Xie, R. Huang and L. Zheng, *Angew. Chem., Int. Ed.*, 2008, **47**, 8901.
47 T. Ming, W. Feng, Q. Tang, F. Wang, L. Sun, J. Wang and C. Yan, *J. Am. Chem. Soc.*, 2009, **131**, 16350.
48 J. Zhang, M. R. Langille, M. L. Personick, K. Zhang, S. Li and C. A. Mirkin, *J. Am. Chem. Soc.*, 2010, **132**, 14012.
49 D. Y. Kim, S. H. Im and O. O. Park, *Cryst. Growth Des.*, 2010, **10**, 3321.
50 Y. Yu, Q. B. Zhang, X. M. Lu and J. Y. Lee, *J. Phys. Chem. C*, 2010, **114**, 11119.
51 H.-L. Wu, C.-H. Kuo and M. H. Huang, *Langmuir*, 2010, **26**, 12307.
52 N. Pazos-Pećrez, S. Barbosa, L. Rodrićguez-Lorenzo, P. Aldeanueva-Potel, J. Pećrez-Juste, I. Pastoriza-Santos, R. A. Alvarez-Puebla and L. M. Liz-Marzaćn, *J. Phys. Chem. Lett.*, 2010, **1**, 24.
53 C. J. Murphy, T. K. Sau, A. M. Gole, C. J. Orendorff, J. Gao, L. Gou, S. E. Hunyadi and T. Li, *J. Phys. Chem. B*, 2005, **109**, 13857.
54 M. Liu and P. Guyot-Sionnest, *J. Phys. Chem. B*, 2005, **109**, 22192.
55 A. Halder and N. Ravishankar, *Adv. Mater.*, 2007, **19**, 1854.
56 Y. Xiong and Y. Xia, *Adv. Mater.*, 2007, **19**, 3385.
57 C. R. Martin, *Science*, 1994, **266**, 1961.
58 A. V. Kabashin, P. Evans, S. Pastkovsky, W. Hendren, G. A. Wurtz, R. Atkinson, R. Pollard, V. A. Podolskiy and A. V. Zayats, *Nat. Mater.*, 2009, **8**, 867.
59 Z. Li, W. Li, P. H. C. Camargo and Y. Xia, *Angew. Chem., Int. Ed.*, 2008, **47**, 9653.
60 Z. Huo, C.-k. Tsung, W. Huang, X. Zhang and P. Yang, *Nano Lett.*, 2008, **8**, 2041.
61 B. Viswanath, Paromita Kundu, Aditi Halder and N. Ravishankar, *J. Phys. Chem. C*, 2009, **113**, 16866.
62 S. Chen, Z. L. Wang, J. Ballato, S. H. Foulger and D. L. Carroll, *J. Am. Chem. Soc.*, 2003, **125**, 16186.
63 E. Hao, R. C. Bailey, G. C. Schatz, J. T. Hupp and S. Li, *Nano Lett.*, 2004, **4**, 327.
64 J. M. Zhu, Y. H. Shen, A. J. Xie, L. G. Qiu, Q. Zhang and S. Y. Zhang, *J. Phys. Chem. C*, 2007, **111**, 7629.
65 J. Gao, C. M. Bender and C. J. Murphy, *Langmuir*, 2003, **19**, 9065.
66 C. J. Murphy, L. B. Thompson, A. M. Alkilany, P. N. Sisco, S. P. Boulos, S. T. Sivapalan, J. A. Yang, D. J. Chernak and J. Huang, *J. Phys. Chem. Lett.*, 2010, **1**, 2867.
67 (*a*) X. S. Kou, S. Z. Zhang, C. K. Tsung, M. H. Yeung, Q. H. Shi, G. D. Stucky, L. D. Sun, J. F. Wang and C. H. Yan, *J. Phys. Chem. B*, 2006, **110**, 16377; (*b*) X. Kou, S. Zhang, C.-K. Tsung, Z. Yang, M. H. Yeung, G. D. Stucky, L. Sun, J. Wang and C. Yan, *Chem. Eur. J.*, 2007, **13**, 2929.
68 T. K. Sau and C. J. Murphy, *J. Am. Chem. Soc.*, 2004, **126**, 8648.
69 W. Niu, S. Zheng, D. Wang, X. Liu, H. Li, S. Han, J. Chen, Z. Tang and G. Xu, *J. Am. Chem. Soc.*, 2009, **131**, 697.
70 J. E. Millstone, W. Wei, M. R. Jones, H. Yoo and C. A. Mirkin, *Nano Lett.*, 2008, **8**, 2526.
71 J. Hu, Y. Zhang, B. Liu, J. Liu, H. Zhou, Y. Xu, Y. Jiang, Z. Yang and Z.-Q. Tian, *J. Am. Chem. Soc.*, 2004, **126**, 9470.
72 (*a*) D. Joseph and K. E. Geckeler, *Langmuir*, 2009, **25**, 13224; (*b*) P. Pallavicini, G. Chirico, M. Collini, G. Dacarro, A. Donà, L. D'Alfonso, A. Falqui, Y. Diaz-Fernandez, S. Freddi, B. Garofalo, A. Genovese, L. Sironi and A. Taglietti, *Chem. Commun.*, 2011, **47**, 1315.
73 A. Mohanty, N. Garg and R. Jin, *Angew. Chem., Int. Ed.*, 2010, **49**, 4962.
74 (*a*) L. Zhong, X. Zhai, X. Zhu, P. Yao and M. Liu, *Langmuir*, 2009, **26**, 5876; (*b*) G. Lin, W. Lu, W. Cui and L. Jiang, *Cryst. Growth Des.*, 2010, **10**, 1118.
75 S. Goy-López, J. Juárez, A. Cambón, J. Botana, M. Pereiro, D. Baldomir, P. Taboada and V. Mosquera, *J. Mater. Chem.*, 2010, **20**, 6808.
76 T. Minami, R. Nishiyabu, M. Iyodab and Y. Kubo, *Chem. Commun.*, 2010, **46**, 8603.
77 N. Zhao and L. Qi, *Adv. Mater.*, 2006, **18**, 359.
78 C. Wang, Y. Hu, C. M. Lieber and S. Sun, *J. Am. Chem. Soc.*, 2008, **130**, 8902.
79 M. N. Nadagouda, G. Hoag, J. Collins and R. S. Varma, *Cryst. Growth Des.*, 2009, **9**, 4979.
80 A. Ali Umar and M. Oyama, *Cryst. Growth Des.*, 2009, **9**, 1146.
81 A. Ali Umar, M. Oyama, M. M. Salleh and B. Y. Majlis, *Cryst. Growth Des.*, 2010, **10**, 3694.
82 A. Douhal, *Chem. Rev.*, 2004, **104**, 1955.
83 (*a*) H. Xing, S.-S. Lin, P. Yan and J.-X. Xiao, *Langmuir*, 2008, **24**, 10654; (*b*) L. Jiang, M. Deng, Y. Wang, D. Liang, Y. Yan and J. Huang, *J. Phys. Chem. B*, 2009, **113**, 7498.
84 X. Zhang and C. Wang, *Chem. Soc. Rev.*, 2011, **40**, 94.
85 X. Lu, M. S. Yavuz, H.-Y. Tuan, B. A. Korgel and Y. Xia, *J. Am. Chem. Soc.*, 2008, **130**, 8900.
86 L. Li, Z. Wang, T. Huang, J. Xie and L. Qi, *Langmuir*, 2010, **26**, 12330.
87 P. Matteini, F. Ratto, F. Rossi, S. Centi, L. Dei and R. Pini, *Adv. Mater.*, 2010, **22**, 4313.
88 T.-R. Kuo, V. A. Hovhannisyan, Y.-C. Chao, S.-L. Chao, S.-J. Chiang, S.-J. Lin, C.-Y. Dong and C.-C. Chen, *J. Am. Chem. Soc.*, 2010, **132**, 14163.
89 O. Vaughan, *Nat. Nanotechnol.*, 2010, **5**, 5.
90 J. Zeng, Q. Zhang, J. Chen and Y. Xia, *Nano Lett.*, 2010, **10**, 30.
91 M. Boronat and A. Corma, *Dalton Trans.*, 2010, **39**, 8538.
92 K. P. McKenna and A. L. Shluger, *J. Phys. Chem. C*, 2007, **111**, 18848.
93 C. Yu and J. Irudayaraj, *Biophys. J.*, 2007, **93**, 3684.
94 M. A. Mahmoud and M. A. El-Sayed, *J. Am. Chem. Soc.*, 2010, **132**, 12704.
95 W. Lu, A. K. Singh, S. A. Khan, D. Senapati, H. Yu and P. C. Ray, *J. Am. Chem. Soc.*, 2010, **132**, 18103.
96 (*a*) P. Zijlstra, James W. M. Chon and Min Gu, *Nature*, 2009, **459**, 410; (*b*) M. Liu, T. Zentgraf, Y. Liu, G. Bartal and X. Zhang, *Nat. Nanotechnol.*, 2010, **5**, 570.
97 M. R. Jones, R. J. Macfarlane, B. Lee, J. Zhang, K. L. Young, A. J. Senesi and C. A. Mirkin, *Nat. Mater.*, 2010, **9**, 913.
98 J. A. Schuller, E. S. Barnard, W. Cai, Y. C Jun, J. S. White and M. L. Brongersma, *Nat. Mater.*, 2010, **9**, 193.
99 H. A. Atwater and A. Polman, *Nat. Mater.*, 2010, **9**, 205.
100 B. Luk'yanchuk, N. I. Zheludev, S. A. Maier, N. J. Halas, P. Nordlander, H. Giessen and C. T. Chong, *Nat. Mater.*, 2010, **9**, 707.

